Fusion Hindrance for a Positive-Q-Value System $^{24}Mg + ^{30}Si$

C. L. Jiang,[1,*] A. M. Stefanini,[2] H. Esbensen,[1] K. E. Rehm,[1] S. Almaraz-Calderon,[1] B. B. Back,[1] L. Corradi,[2] E. Fioretto,[2] G. Montagnoli,[3] F. Scarlassara,[3] D. Montanari,[3] S. Courtin,[4] D. Bourgin,[4] F. Haas,[4] A. Goasduff,[5] S. Szilner,[6] and T. Mijatovic[6]

[1]*Physics Division, Argonne National Laboratory, Argonne, Illinois 60439, USA*
[2]*INFN, Laboratori Nazionali di Legnaro, I-35020 Legnaro (Padova), Italy*
[3]*Dipartimento di Fisica e Astronomia, Universitá di Padova, and INFN, Sezione di Padova, IT-35131 Padova, Italy*
[4]*IPHC and University of Strasbourg, CNRS/IN2P3,67037 Strasbourg Cedex2, France*
[5]*CSNSM, CNRS/IN2P3 and University Paris-Sud, F-91405 Orsay Campus, France*
[6]*Ruder Boskovic Institute, HR-10002 Zagreb, Croatia*

(Received 2 May 2014; published 10 July 2014)

Measurements of the excitation function for the fusion of $^{24}Mg + ^{30}Si$ ($Q = 17.89$ MeV)have been extended toward lower energies with respect to previous experimental data. The S-factor maximum observed in this large, positive-Q-value system is the most pronounced among such systems studied thus far. The significance and the systematics of an S-factor maximum in systems with positive fusion Q values are discussed. This result would strongly impact the extrapolated cross sections and reaction rates in the carbon and oxygen burnings and, thus, the study of the history of stellar evolution.

DOI: 10.1103/PhysRevLett.113.022701 PACS numbers: 25.70.Jj, 97.10.Cv, 97.10.Tk

The phenomenon of heavy-ion fusion hindrance at extreme low energies was discovered about 10 years ago [1–4]. The experimental evidence was at first observed for medium-heavy systems, for which fusion Q values are negative. A characteristic behavior is that there is an S-factor maximum appearing at deep sub-barrier energies, which is not expected by the standard coupled-channels (CC) predictions but is required from the principle of energy conservation [5]. Later, the suppression of the fusion probability at low energies was explained successfully in terms of the saturation properties of nuclear matter [6]. The recipe to describe this effect is the inclusion of a repulsive core in the nuclear potential. Another successful description is the development of an adiabatic model [7], which realizes the suppression of the fusion probability by decreasing the coupling strength after the touching of the two colliding nuclei.

For a system with a positive fusion Q value, it is not necessary to have an S-factor maximum, since energy conservation allows for a finite cross section at zero incident energy. The first observation of hindrance in lighter fusion systems with positive Q values was obtained in a systematic study of the logarithmic derivative, $L(E) = dln(\sigma E)/dE$, over a wide mass range of fusion systems [8]. However, assuming that the reason for hindrance is the saturation properties of nuclear matter or the decrease of the coupling strength after the contact of two colliding nuclei, it is expected that the fusion hindrance must also appear for light heavy-ion fusion [9].

Deep sub-barrier fusion between carbon and oxygen nuclei, which also have positive fusion Q values, plays a decisive role in high density, high temperature stellar environments. This work therefore has a direct impact on the description of these astrophysical process by providing more reliable recipes for extrapolation of the relevant cross sections and reaction rates into the temperature range of interest.

While fusion hindrance has been observed in many heavy-ion fusion reactions with positive Q values, the behavior in these systems at very low energies is still not well established. It should be noted that all previous model calculations and extrapolation recipes predict that the S factor increases when the energy decreases. It is therefore of great interest to determine whether a maximum in the S factor also occurs for positive-Q-value systems, since it would have important consequences for the rate of astrophysical fusion processes. Because cross-section measurements in the critical energy windows for carbon and oxygen burning are still unattainable in the laboratory, extrapolations to lower energies must be used in simulation calculations, which will be strongly influenced by the fusion hindrance. In addition to the persistent experimental efforts to extend the measurements for fusion of $^{12}C + ^{12}C$ towards lower energies, measurements for slightly heavier, positive-Q-value systems have been pursued in order to understand the fusion behavior at deep sub-barrier energies.

In recent years, fusion excitation functions of five positive-Q-value systems, $^{28}Si + ^{30}Si$ ($Q = 14.3$ MeV) [10], $^{27}Al + ^{45}Sc$ ($Q = 9.63$ MeV) [11], $^{40}Ca + ^{48}Ca$ ($Q = 4.56$ MeV) [12], $^{36}S + ^{64}Ni$ ($Q = 7.66$ MeV) [13], and $^{36}S + ^{48}Ca$ ($Q = 7.55$ MeV) [14], together with their neighboring systems of negative Q values, $^{40}Ca + ^{40}Ca$ ($Q = -14.2$ MeV) [15], $^{48}Ca + ^{48}Ca$ ($Q = -2.99$ MeV) [16], $^{28}Si + ^{64}Ni$ ($Q = -1.79$ MeV) [17], and $^{36}S + ^{64}Ni$

($Q = -8.54$ MeV) [18], have been measured or remeasured to lower energies for this purpose. Indications of fusion hindrance have been observed in all cases since these excitation functions drop faster than predicted by the CC calculations with a standard Woods-Saxon potential. Only in the ^{40}Ca + ^{48}Ca system has an S-factor maximum been observed, but it does not show up very clearly [12]. In many cases, various background processes prevent the measurements from being extended to sufficiently low cross sections.

In order to investigate this question further, we have remeasured the fusion excitation function for the system ^{24}Mg + ^{30}Si ($Q = 17.89$ MeV), which was previously measured down to cross sections of 73 μb by Morsad *et al.* [19], already into the region where fusion hindrance plays an important role.

The experiment was performed at the XTU Tandem accelerator of Laboratori Nazionali di Legnaro of INFN, Italy. A ^{24}Mg beam of 5—10 pnA bombarded a SiO_2 target with thickness ~30 $\mu g/cm^2$ (evaporated onto a 20 $\mu g/cm^2$ carbon backing). The isotopic abundance of ^{30}Si was 96.78%. The evaporation residues were detected with an electrostatic separator in its upgraded configuration [13]. The detector system consists of two microchannel plate detectors, one ionization chamber, and a silicon surface-barrier detector. Details of the experimental setup and the data analysis have been described elsewhere; see Refs. [3,14,16,20].

The main objective was a study of the hindrance behavior in the low-energy region. All together, measurements were taken at seven energies, five of them coinciding with the previous measurements as shown in Table I. Events of evaporation residues were well separated from the background in the present experiments even at the lowest measured energy. Five parameters, namely, the residual energy in silicon detector E_R, the energy loss in the ionization chamber ΔE, and three time-of-flight signals (t_1, t_2, and t_3) were recorded and used to select the fusion events. In Fig. 1, the time-of-flight signals t_1, t_2, t_3 and ΔE versus E_R are shown for the fusion events collected in the measurements at the four lowest energies.

Our measurements were normalized to the cross sections of Morsad *et al.* at four energies. Thus, we obtain one refined and two new data points at low energies. All energies E indicated in this Letter are for the center-of-mass system. The cross section for the lowest energy in Ref. [19] at 21.1 MeV was derived from three fusion events having a statistical uncertainty of 58%. At the three lowest energies in the present experiment, the cross sections obtained correspond to 11, 11, and 4 events, respectively. The present experimental results are given in Table I and compared with the ones from Ref. [19].

The experimental excitation function for the system ^{24}Mg + ^{30}Si is presented in Fig. 2. The green circles are the present results, and the black open circles are from

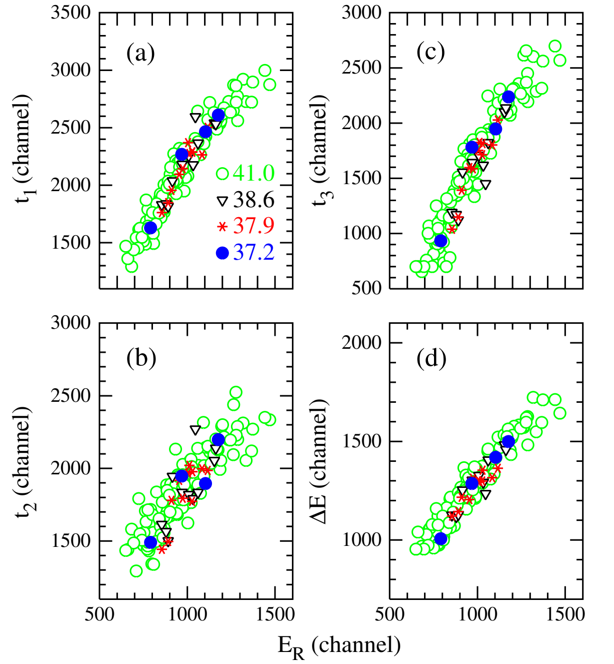

FIG. 1 (color online). Fusion events collected in the measurements at the four lowest energies (green open circles, black open triangles, red stars, and blue circles, respectively) in the spectra of t_1, t_2, t_3 versus E_R (a)–(c) and ΔE versus E_R (d).

Ref. [19]. The uncertainties of the present data are determined from the statistics and the normalization procedure.

Experimental results of the S factor and the logarithmic derivative are shown in Figs. 3(a) and 3(b). In the logarithmic derivative representation, the experimental $L(E)$ exceeds the constant S-factor curve, $L_c(E) = \pi\eta/E$ [1]. Thus, there is an S-factor maximum with a limit at $E = 20.8$ MeV, although further improvements in the data are desirable. Nevertheless, this result is more convincing than the previous one, the first evidence in a positive-Q-value system ^{40}Ca + ^{48}Ca [12],

In the study of the hindrance behavior, an extrapolation recipe for systems with a positive fusion Q value was developed in Ref. [9]. From a fit of the logarithmic derivative $L(E)$ in the low-energy region with the expression

TABLE I. Cross sections measured in the present experiment and compared with the data of Morsad *et al.* [19].

E(MeV)	σ (mb), present	σ (mb), Ref. [19]
28.5	327(24)	332(24)
26.3	161(13)	179(13)
24.1	38.2(2.9)	41.4(2.9)
22.4	2.53(0.26)	2.12(.22)
21.1	0.088(0.027)	0.073(0.042)
20.68	0.035(0.011)	
20.29	0.0080(0.0040)	

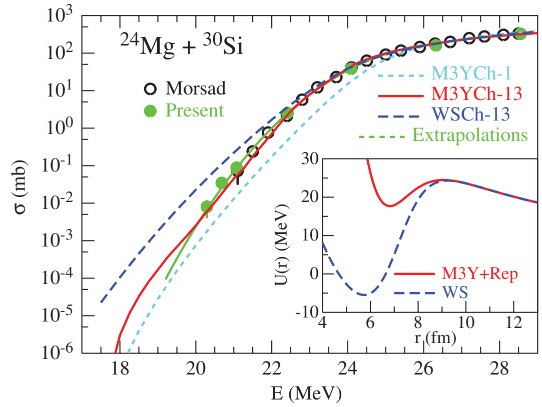

FIG. 2 (color). Excitation functions of ^{24}Mg + ^{30}Si, as measured by Morsad *et al.* (black open circles) [19] and in the present experiment (green circles). The lines are from calculations (see text for details). The inset shows the radial shape of the potentials.

$$L(E) = A_0 + B_0/E^{3/2}, \tag{1}$$

the extrapolated excitation function is given by

$$\sigma(E) = \sigma_s \frac{E_s}{E} e^{\{A_0(E-E_s)-B_0[2/E_s^{1/2}][(E_s/E)^{1/2}-1]\}}. \tag{2}$$

Here E_s is the energy of the crossing point of Eq. (1) with the constant S-factor function, $\pi\eta/E$, i.e., the location of the S-factor maximum. A_0, B_0, and σ_s are fit parameters. The green curves in Figs. 2 and 3 are the extrapolations obtained with Eq. (1), $E_s = 20.8$ MeV, $A_0 = -6.71$ MeV^{-1}, $B_0 = 939$ MeV$^{1/2}$, and $\sigma_s = 0.0363$ mb. It should be noted that by including only the data from Ref. [19] in the fit, the parameters obtained are nearly identical to the values obtained from a fit to all data points. This indicates that the extrapolations from the data of Morsad *et al.* can predict the new measurements at lower energies. Thus, it appears that extrapolations using Eq. (1) are robust.

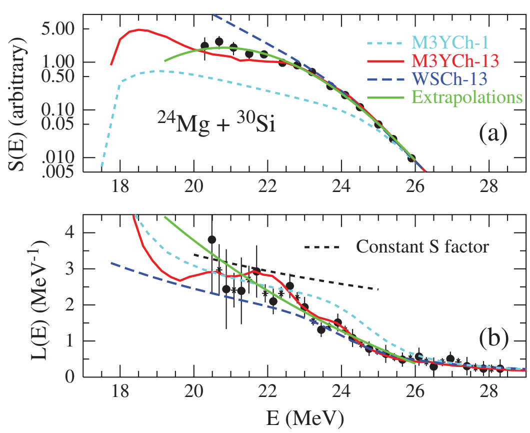

FIG. 3 (color). $S(E)$ factors (a) and logarithmic derivatives $L(E)$ (b) for ^{24}Mg + ^{30}Si. A clear S-factor maximum is exhibited.

Coupled-channels calculations are also shown in Figs. 2 and 3. The CC calculation with a standard Woods-Saxon potential provides an excellent description of the data above the Coulomb barrier and is presented as blue long-dashed curves (WSCh-13). The parameters used are $U_0 = 52.74$ MeV, $a = 0.63$ fm, and $R = 7.15$ fm. At lower energies, it overpredicts the experimental data, which gives strong evidence of fusion hindrance. With the combination of a M3Y potential and a repulsive core (M3Y + Rep), CC calculations describe rather well the experimental result over the whole energy range. In particular, they reproduce the hindrance behavior and an S-factor maximum as represented by the red curve, M3YCh-13, though at an energy lower than the observation.

The M3Y + Rep potential was constructed as described in Ref. [6] from the nuclear densities of the reacting nuclei that were parametrized as Fermi functions with diffuseness $a = 0.52$ and 0.48 fm and radius $R = 3.032$ and 3.13 fm, respectively, for ^{24}Mg and ^{30}Si. These radii were adjusted to optimize the fit to the fusion data, whereas the repulsive part of the potential was determined by the nuclear incompressibility $K = 234$ MeV. The entrance-channel potential thus determined is compared to the Woods-Saxon potential in the inset of Fig. 2. The CC calculations are similar to those that were performed in Refs. [4,15]. They include the one- and two-phonon excitations, as well as mutual excitations of the 2^+ and 3^- states in projectile and target, excluding though the two-phonon excitations of the two 3^- states. That gives a total of 13 channels referred to as M3YCh-13. The effective two-phonon excitations of the 2^+ states were constructed from the measured transitions from the 0_2^+, 2_2^+, and 4_1^+ to the 2_1^+ one-phonon state as described in Ref. [21]. The detailed information that goes into this construction for ^{24}Si and ^{30}Si is shown in Table II. Calculations denoted as M3YCh-1 are the results when no coupling effect is included (light blue dashed line).

TABLE II. The states of ^{24}Mg and ^{30}Si included in the CC calculations [22,23].

Nucleus	λ^π	E_x (MeV)	$B(E\lambda)(W.u.)$	β_λ^C	β_λ^N
^{24}Mg	2^+	1.369	21.2	0.608	0.460
0–2	0^+				
2—2	2^+	4.238	3.12		
2—4	4^+	4.123	36		
	2PH(2^+)	4.128	19.4	0.41	0.32
	3^-	7.616	4.7	0.28	0.28
^{30}Si	2^+	2.235	8.5(11)	0.330	0.330
0—2	0^+	3.787	1.4		
2–2	2^+	3.499	9(6)		
4—2	4^+	5.279	4.7(13)		
	2PH(2^+)	4.331	5.2	0.184	0.184
	3^-	5.487	6.1	0.275	0.275

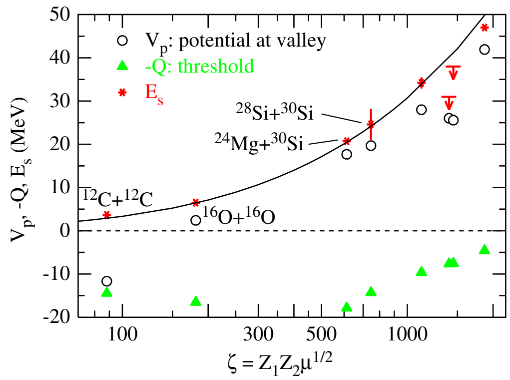

FIG. 4 (color online). Plot of the potential pocket values, V_p of the M3Y+Rep potential (black open circles), threshold energy $-Q$ (green triangles) and E_s (red stars) versus entrance parameter $\zeta = Z_1 Z_2 \sqrt{\mu}$.

There are very different minimum values at the potential pocket V_p, −5.5 and 17.7 MeV for WS and M3Y + Rep, respectively. The fusion is simulated by ingoing wave boundary conditions that are imposed at the minimum of the pocket in the entrance-channel potential. That implies that the fusion cross section will be zero when the center-of-mass energy is smaller than the minimum of the pocket in the entrance-channel potential. In the case of the M3Y + Rep potential, this occurs at 17.7 MeV and is exhibited in both the M3YCh-13 and M3YCh-1 calculations. We have collected the pocket values V_p of the M3Y + Rep potential for the calculations on systems with positive fusion Q value. A plot of V_p versus an entrance-channel parameter $\zeta = Z_1 Z_2 \sqrt{\mu}$ (where μ is the reduced mass) is presented in Fig. 4 (black open circles), together with the threshold energy $-Q$ (green triangles) and the values E_s [energy location of the maximum, obtained from the recipe of Eq. (1), red stars]. In the figure, lighter systems $^{12}C + ^{12}C$ [9,24] and $^{16}O + ^{16}O$ [25] are also included. In the order of increasing ζ, the systems at $\zeta > 1000$ are $^{27}Al + ^{45}Sc$, $^{32}S + ^{48}Ca$, $^{36}S + ^{48}Ca$, and $^{40}Ca + ^{48}Ca$. We find that, except for the system $^{12}C + ^{12}C$, all V_p values in Fig. 4 are positive. For these systems the fusion cross sections should go to zero when the energy reaches V_p. Accordingly, there should be an S-factor maximum located at an energy higher than V_p. For $^{12}C + ^{12}C$, the V_p of this model is negative, and no conclusion can be drawn about the S-factor maximum. In the study of Ref. [9], by using the extrapolation recipe described above, an intersection between the $L(E)$ and the constant S-factor function for the system $^{12}C + ^{12}C$ is observed, which implies that there would be an S-factor maximum. In the systematics study of $L(E)$ [8], it was mentioned that, for an even lighter system, e.g., $^{10}B + ^{10}B$, the $L(E)$ at low energies are nearly parallel with the constant S-factor function. The behavior for these very light systems at very low energies is unknown.

If the saturation properties of nuclear matter, as computed with the M3Y + Rep model, is a valid description of the hindrance behavior, it would introduce a strong inhibition of the fusion process at energies corresponding to the pocket in the potential. As a result, there should also be an S-factor maximum for positive-Q-value systems at least as light as $^{16}O + ^{16}O$. These observations would have a large influence on the reaction rates of carbon and oxygen burning at low energies. Gasques *et al.* studied the implications of low-energy fusion hindrance on stellar burning and nucleosynthesis [26]. They concluded that the modifications, when the fusion hindrance is included, will require much higher ignition densities for, e.g., white dwarf supernovae, and will change the abundance of many isotopes in massive late-type stars.

The black curve in Fig. 4 is obtained from the phenomenological study of E_s [27]:

$$E_s^{emp} = [0.495\zeta / L_s^{emp}(\zeta)]^{2/3} (\mathrm{MeV}), \qquad (3)$$

with $L_s^{emp}(\zeta) = 2.33 + 580/\zeta$. The E_s obtained from $^{24}Mg + ^{30}Si$ agrees with the systematics. It is interesting to point out that the V_p values, except for $^{12}C + ^{12}C$, are nearly parallel with the E_s values (and E_s^{emp} curves) as shown in Fig. 4. That observation may help to understand the character of the saturation properties of nuclear matter.

In summary, the fusion excitation function of $^{24}Mg + ^{30}Si$ has been extended to lower energies. An S-factor maximum has been observed for a large positive-Q-value system, which is the best developed maximum observed thus far. This observation implies that the cross section falls off very steeply at even lower energies. By extension, we may expect that similar precipitous reduction in the cross sections occurs for other positive Q-value systems, such as those involved in the carbon phase of giant stars. The energy at the maximum $E_s = 20.8$ MeV falls on the phenomenologic curve E_S^{emp}. A collection of the pocket values V_p of the potentials obtained from the calculations of the M3Y + Rep model for these positive fusion Q-value systems shows that there may be an S-factor maximum for systems at least as light as $^{16}O + ^{16}O$. This character would introduce a strong influence on the predictions of the reaction rates that are important in the study of the history of stellar evolution.

This work was supported by the U.S. Department of Energy, Office of Nuclear Physics, under Contract No. DE-AC02-06CH11357, and the European Union Seventh Framework Programme FP7/2007-2013 under Grant Agreement No. 262010-ENSAR. A. G. was partially supported by the P210 Excellence Laboratory.

*jiang@phy.anl.gov

[1] C. L. Jiang *et al.*, Phys. Rev. Lett. **89**, 052701 (2002); Phys. Rev. Lett. **93**, 012701 (2004).

[2] M. Dasgupta, D. J. Hinde, A. Diaz-Torres, B. Bouriquet, C. I. Low, G. J. Milburn, and J. O. Newton, Phys. Rev. Lett. **99**, 192701 (2007).
[3] A. M. Stefanini *et al.*, Phys. Rev. C **82**, 014614 (2010).
[4] B. B. Back, H. Esbensen, C. L. Jiang, and K. E. Rehm, Rev. Mod. Phys. **86**, 317 (2014).
[5] C. L. Jiang, H Esbensen, B. B. Back, R. V. F. Janssens, and K. E. Rehm, Phys. Rev. C **69**, 014604 (2004).
[6] Ş. Mişicu and H. Esbensen, Phys. Rev. Lett. **96**, 112701 (2006); Phys. Rev. C **75**, 034606 (2007).
[7] T. Ichikawa, K. Hagino, and A. Iwamoto, Phys. Rev. C **75**, 057603 (2007); Phys. Rev. Lett. **103**, 202701 (2009); T. Ichikawa and K. Matsuyanagi, Phys. Rev. C **88**, 011602(R) (2013).
[8] C. L. Jiang, B. B. Back, H Esbensen, R. V. F. Janssens, and K. E. Rehm, Phys. Rev. C **73**, 014613 (2006).
[9] C. L. Jiang, K. E. Rehm, B. B. Back, and R. V. F. Janssens, Phys. Rev. C **75**, 015803 (2007).
[10] C. L. Jiang *et al.*, Phys. Rev. C **78**, 017601 (2008).
[11] C. L. Jiang *et al.*, Phys. Rev. C **81**, 024611 (2010).
[12] C. L. Jiang *et al.*, Phys. Rev. C **82**, 041601(R) (2010).
[13] G. Montagnoli *et al.*, Phys. Rev. C **87**, 014611 (2013).
[14] A. M. Stefanini *et al.*, Phys. Rev. C **78**, 044607 (2008).
[15] G. Montagnoli *et al.*, Phys. Rev. C **85**, 024607 (2012).
[16] A. M. Stefanini *et al.*, Phys. Lett. B **679**, 95 (2009).
[17] C. L. Jiang *et al.*, Phys. Lett. B **640**, 18 (2006).
[18] G. Montagnoli, A. M. Stefanini, L. Corradi, S. Courtin, E. Fioretto, F. Haas, D. Lebhertz, F. Scarlassara, R. Silvestri, and S. Szilner, Phys. Rev. C **82**, 064609 (2010).
[19] A. Morsad, J. J. Kolata, R. J. Tighe, X. J. Kong, E. F. Aguilera, and J. J. Vega, Phys. Rev. C **41**, 988 (1990)
[20] A. M. Stefanini *et al.*, Phys. Rev. C **81**, 037601 (2010).
[21] H. Esbensen, Phys. Rev. C **72**, 054607 (2005).
[22] NNDC/ENSDF, Brookhaven National Laboratory, www.nndc.bnl.gov/ensdf.
[23] M. Mittag, P. Charles, S. M. Lee, I. Badewy, B. Berthier, B. Femandez, and J. Gastebois, Nucl. Phys. **A233**, 48 (1974).
[24] H. Esbensen, X. Tang, and C. L. Jiang, Phys. Rev. C **84**, 064613 (2011).
[25] H. Esbensen, Phys. Rev. C **77**, 054608 (2008).
[26] L. R. Gasques, E. F. Brown, A. Chieffi, C. L. Jiang, M. Limongi, C. Roafs, M. Wiescher, and D. G. Yakovlev, Phys. Rev. C **76**, 035802 (2007).
[27] C. L. Jiang, K. E. Rehm, B. B. Back, and R. V. F. Janssens, Phys. Rev. C **79**, 044601 (2009).